Lasers in Manufacturing Conference 2019

A theoretical model for reactive gas laser cutting of metals

M. H. Brügmann[a*], M. Muralt[b], B. Neuenschwander[b], S. Wittwer[c], T. Feurer[a]

[a]*Institute of Applied Physics, University of Bern, Sidlerstrasse 5, CH-3012 Bern, Switzerland*
[b]*BFH Burgdorf, Pestalozzistrasse 20, CH-3400 Burgdorf, Switzerland*
[c]*Bystronic AG., Industriestrasse 21, CH-3362, Niederönz, Switzerland*

Abstract

We present a theoretical model for the process of reactive gas laser cutting of metals with emphasis on the roughness profile of the cutting edges, i.e. striation. Theoretical results are verified against experimental observations for 10 mm DD11 steel plates. Striation spectra were obtained by performing a numerical Fourier transform of the measured roughness profiles. The spectra were then fitted to those of a driven damped harmonic oscillator yielding information on amplitudes, resonance frequencies and damping constants. These parameters were determined for different focal positions and cutting speeds. Generally, we find a good agreement between the theoretical model and experiment. From this we conclude that our model is able to predict important quality parameters of reactive gas laser cutting and how to optimize them.

Keywords: Macro-Processing ; Cutting; Fundamentals and Process Simulation

* Corresponding author. Tel.: +41-316-318-934
E-mail address: michael.bruegmann@iap.unibe.ch

1. Introduction

Laser cutting is one of the most widely used Laser Beam Machining processes. Among the materials, that exhibit favorable thermal and optical properties for laser cutting, we find metals. Therefore, the laser cutting process is well suited for cutting of metal plates. However, there are several side effects that limit the quality of the process. One of the main limitations is the formation of a typical roughness pattern at the edges that has the form of periodic striations. In different publications these striations are also called grooves, strokes or patterns [1], [2], [3]. Since striations strongly affect the quality of the laser cut many experimental and theoretical studies on the mechanisms of striation formation were conducted [4], [5], [6], [7], [1], [2], [3], [8].

1.1. The reactive gas laser cutting process

In the process of reactive gas laser cutting a high power continuous wave laser beam is focused to a spot on a workpiece where it melts the metal. Additionally, a nozzle supplies a high pressure reactive assist gas in order to 1) remove the molten material from the melting pool and 2) add energy via chemical reaction between gas and molten material. In practice oxygen is widely used as assist gas. The heterogeneous chemical reaction of iron oxidation with the accompanied release of heat in the laser pool will take place primarily at the cutting front. The added process energy allows for an almost threefold increase in cutting speed as compared with cutting in an inert gas environment (argon, helium or nitrogen) [9], [3].

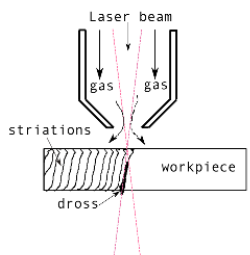

Fig. 1. Schematic of laser cutting.

The chemical reaction of iron oxidation in oxygen atmosphere result in a complex interplay of many processes, i.e. in periodic cycles of ignition, combustion and decay. The reaction rates themselves are controlled by heat- and mass-transfer between the gaseous, liquid and solid phases of the metal. As a consequence, the cut surface develops roughness and deep striations. Theoretical analysis of the mechanisms of striation formation in reactive gas laser cutting were, for example, performed in [6], [7], [2] and [3]. In many cases [6], [7], [1], [2], the modelling of striation formation was based on the theory of hydrodynamic instabilities in the molten layer. Here, we present a theoretical model for striation formation in reactive gas laser cutting which is developed starting from the analysis presented in [6] and [7].

2. Theoretical modelling

In References [6], [7], by using dynamic energy and mass balance equations, it was shown that the striation formation in reactive gas laser cutting can be modelled by an equation of the type of a driven damped oscillator for the first order perturbations δs of the stationary molten layer thickness s_0

$$\frac{d^2(\delta s)}{dt^2} + \alpha \frac{d(\delta s)}{dt} + \omega_0^2(\delta s) = \frac{F}{m} e^{j\omega t}, \tag{1}$$

where $\delta s = \delta s(t)$ is the first order perturbation of the stationary molten layer thickness s_0. In this case, the undamped oscillation frequency ω_0 and damping constant α are complex functions of material constants, thermal constants, molten layer thickness s_0, cut kerf width, workpiece thickness, molten layer temperature, derivative of the mass losses per unit time with respect to the temperature and molten layer thickness as well as the derivative of the power losses with respect to the temperature. The term $(F/m)e^{j\omega t}$ is a complex function of laser power, reactive power arising from oxidation, material constants, thermal constants and derivative of the mass losses per unit time with respect to the temperature.

The explicit expressions for ω_0, α and $(F/m)e^{j\omega t}$ are given in [7]. The solution of eq. (1) reads

$$\delta s(t) = \delta e^{j\omega t} \tag{2}$$

with

$$\delta = \frac{A_0}{\sqrt{\left(\omega^2 - \omega_0^2\right)^2 + \omega^2\, \alpha^2}} \tag{3}$$

By virtue of equations (1) and (3) the molten layer oscillation is modelled by the equation of a driven harmonic oscillator whose resonance frequency is given by

$$\omega_R = \omega_0 \sqrt{1 - \left(\frac{1}{2}\right)\left(\frac{\alpha}{\omega_0}\right)^2} \quad . \tag{4}$$

Here, it is important to point out that in the case that $\alpha << \omega_0$, the resonance frequency can be approximated by

$$\omega_R \approx \omega_0. \tag{5}$$

In order to adapt the oscillator model to striation formation, we developed a procedure to determine the values of the derivatives of mass losses per unit time with respect to the temperature and molten layer thickness. Our procedure is based on balance equations for mass and power, information on kerf geometry and hydrodynamics of the molten layer. The oscillating molten layer causes a spatially periodic distortion of the cut edges. The wavelength of that distortion is given by (see Refs [6], [7] and references therein),

$$\lambda = \frac{2\pi\, v_c}{\omega_R}, \tag{6}$$

where v_c is the cutting speed and ω_R is given by eq. (4).

3. Theoretical model versus experiment

In order to test the quality of our theoretical model we compare the calculated values for striation frequencies, damping constants and striation amplitudes with the corresponding measured quantities obtained from different experiments.

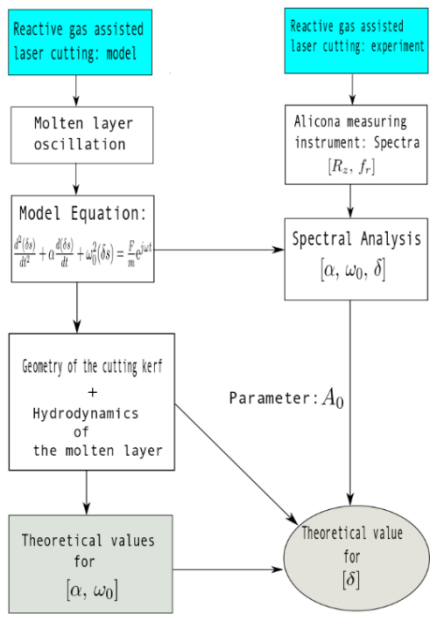

Fig. 2. Diagram.

In order to illustrate the path that we have followed in the validation process of our model, we refer to the diagram depicted in figure 2. On the left-hand side of the diagram we depict different elements of the model as well as quantities that can be calculated directly from it, e.g. the oscillator frequency ω_0 and the damping constant α. On the right-hand side of the diagram we depict the elements corresponding to the experimental part. Here, the mean roughness R_z as well as the spatial striation frequency f_r are quantities that were obtained from measurements. The arrows between the left and right hand sides indicate the elements of the theoretical model that are used in the analysis of the experimental data. For example, we used the equation for a damped driven oscillator as model equation in the spectral analysis. From the spectral analysis we obtained experimental values for the oscillator frequency ω_0, the damping constant α and the oscillation-amplitude δ. Here, it is important to mention that the oscillation-amplitude is linked to the mean roughness R_z. On the other hand, the theoretical value for the oscillation amplitude δ can be calculated only by combining the theoretical modelling with the experiment, i.e. after determining the value of the parameter A_0 from specifically tailored measurements.

4. Analysis of the striation spectra

In this section we calculate the striation frequencies as well as the damping constants from the measured striation spectra. In order to calculate these quantities we proceeded in the following way. We load the spectra data in a MATLAB program and perform a fit of the spectra to a Lorentzian line shape (taking into account the basic equations (1) to (3) of our theoretical model)

$$f(\omega) = \frac{A_0}{\sqrt{\left(\omega^2 - \omega_0^2\right)^2 + \omega^2\,\alpha^2}} + B_0, \tag{7}$$

B_0 accounts for white noise. From the fit we extract the model parameters A_0, ω_0, α and B_0 and calculate the corresponding maximal amplitude δ_{max} of the striation by applying equation

$$\delta_{max} = f(\omega_R) - B_0, \tag{8}$$

where

$$f(\omega_{R)} = \frac{A_0}{\alpha\omega_0\sqrt{1-(\frac{1}{4})(\frac{\alpha}{\omega_0})^2}} + B_0. \tag{9}$$

Finally, in order to compare the values of the maximal amplitude with the measured roughness values, we have to add to δ_{max} the value of the background B_0, i.e. the noise in the measurement. The reason for this is that the different experimentally determined roughness values, i.e. R_z, R_a, R_q, etc. are contaminated with noise.

5. Results and Discussion

In this section we present the results regarding the spatial frequencies, damping constants and amplitudes of the striations obtained from the measured spectra. Whereas in the first part we present an analysis of these quantities as function of the focal position of the laser with respect to the workpiece, the second part is devoted to the analysis of the values arising from experiments in which the cutting speed was varied.

5.1. Striation amplitude and damping constant as function of the focal position

In figures 3 and 4 the spectra for the different values of the focal position z_0 are depicted. In every spectrum the presence of a resonance frequency peak is clearly seen. This peak corresponds to the resonance frequency ω_R as given in eq. (4). It is related to the striation wavelength by virtue of equation (6). From figures 3 and 4, we also see that the signal-to-noise-ratio (SNR) is lower for higher focal positions, i.e. for z_0=-4.5 mm or z_0=-6.50 mm[†]. In the case of the spectrum corresponding to z_0=-9.5 mm we see also a much smaller secondary resonance frequency peak at a frequency of $2\omega_R$. This frequency peak is related to

[†]Note, that in our reference system a negative value of the focal position corresponds to the focus of the laser being above the workpiece. If the focus is at the top surface of the workpiece, the corresponding focal position is zero and positive below.

the striations from the transition region between upper and bottom part of the kerf sidewalls. It is known from previous research [10], [11] that the frequency of striations at the transition zone is two times higher with respect to that of the ripples at the upper part of the kerf. Here, it is also important to mention that the spectra correspond to roughness measurements that were carried out at a line on the side walls of the kerf located 5 mm below the top edge. The laser power and cutting speed were fixed at PL=5000 W and v_c=2.1 m/min respectively.

Figure 5(a) shows the spatial oscillation frequency calculated from the spectra and the measured spatial frequencies as function of the focal position. Figure 5(a) indicates that the agreement between measured and calculated values is very good. In figure 5(b) the values for damping constant obtained from the spectral analysis are plotted as function of the focal position. From the plot it can be seen that the value of the damping constant increases when the value of the focal position increases, i.e. when the focal position is placed closer to the top edge of the workpiece.

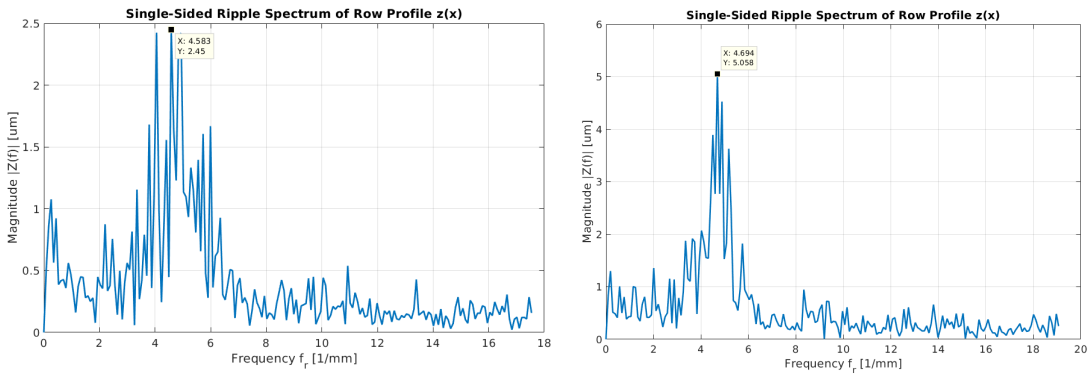

Fig. 3. (a) Spectrum for z0=-4.5 mm; (b) Spectrum for z0=-6.5 mm.

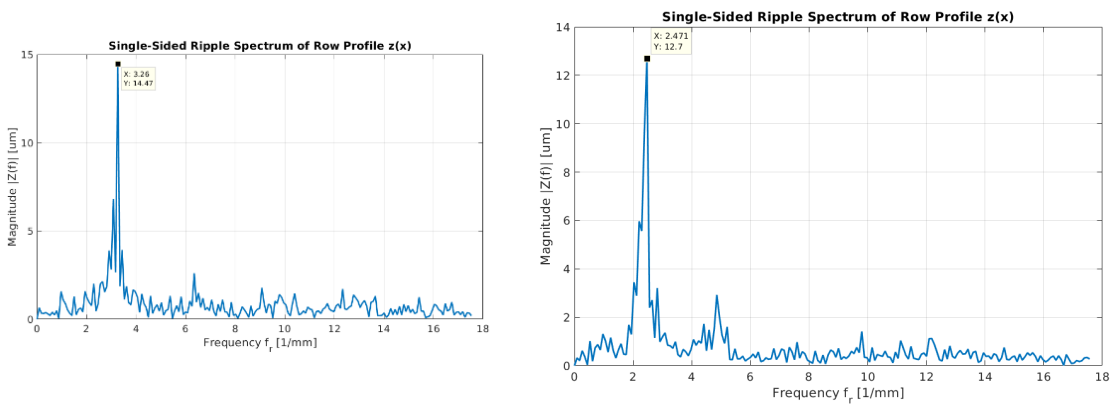

Fig. 4. (a) Spectrum for z0=-8.0 mm; (b) Spectrum for z0=-9.5 mm.

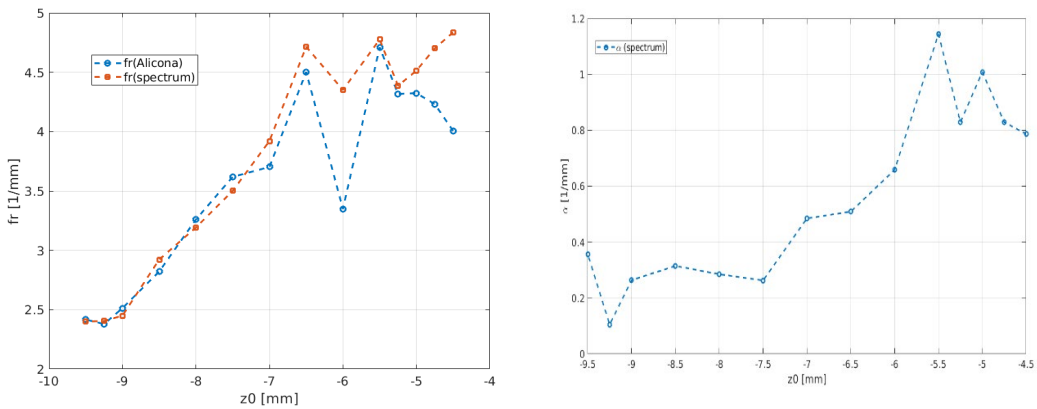

Fig. 5. (a) Striation spatial frequency; (b) Damping constant.

Figure 6(a) shows the striation amplitude as function of the focal position. The striation amplitude is represented in this case on the one hand by profile roughness parameters such as the mean roughness R_z and the mean square roughness amplitude R_q. Both are obtained directly from the roughness profile. On the other hand the striation amplitude is represented by the amplitude δ that is obtained from the striation spectrum.

Figure 6(a) indicates that the three amplitudes decrease when the value of the focal position is increased, i.e. when the focal position is placed closer to the top edge of the workpiece. Also, the values of R_q and δ are of the same order whereas the values of R_z are 3 to 4 times larger. Here, it is also worthwhile to point out that the decrease of the striation amplitudes with increasing focal position is linked to an increase of the damping constant as seen in figure 5(b). This fact is consistent with the driven harmonic oscillator model and it is a strong hint that the striation dynamics can be explained by the model.

In figure 6(b) the striation amplitudes represented by the values of R_q, δ and δ (model-formula) are depicted as function of the focal position. The value of δ was obtained from the striation spectrum by applying the equation (3). The value of A_0 was obtained from spectral analysis.

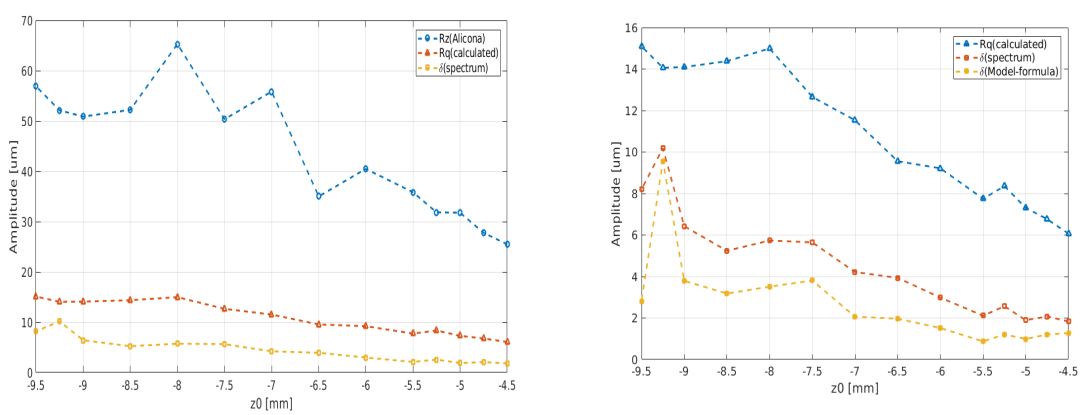

Fig. 6. (a) Striation amplitude as function of the focal position; (b) Striation amplitude as function of the focal position.

5.2. Striation amplitude and damping constant as function of cutting speed

Figure 7 depicts the spectra for different values of the cutting speed v_c. As for the different focal positions, here the spectra also show a resonance frequency peak which corresponds to the resonance frequency ω_R in equation (4). In all spectra in figure 7 we see also a much smaller secondary resonance frequency peak at a frequency of $2\omega_R$. As we explained before this frequency peak is linked to the striations at the transition zone between upper and lower part of the kerf sidewalls. Here, the spectra correspond to roughness measurements that were carried out along a line on the side walls of the kerf located 5 mm below the top edge. In this case, laser power and focal position were fixed at PL=5000 W and z0=-6.5 mm, respectively.

Figure 8(a) shows the spatial oscillation frequency calculated from the spectra and the measured spatial frequencies as function of the cutting speed. Figure 8(a) indicates that the agreement between measured and calculated values is very good. In figure 8(b) the values for the damping constant obtained from the spectral analysis are plotted as function of the cutting speed. From the plot it can be seen that the value of the damping constant increases with cutting speed. To the decrease of the oscillation amplitude and the $\underline{R_z}$-value with increasing cutting speed corresponds an increase of the damping constant as confirmed by figure 8(b).

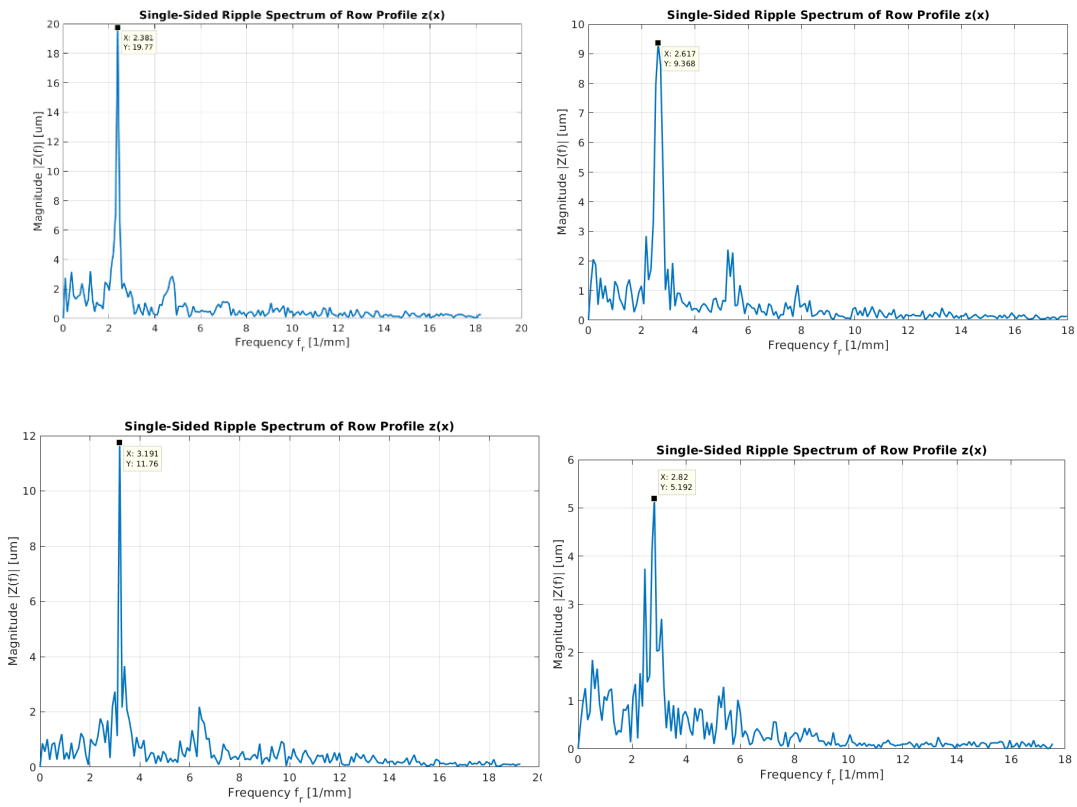

Fig. 7. (a) Spectrum for v_c = 1.4 m/min; (b) Spectrum for v_c =1.7 m/min; (c) Spectrum for v_c =2 m/min; (d) Spectrum for v_c = 2.3 m/min.

Figure 9(a) shows the striation amplitude as function of the cutting speed. As before, the striation amplitude is represented by profile roughness parameters such as the mean roughness R_z and the mean square roughness amplitude R_q. Both are obtained directly from the roughness profile. The striation amplitude δ is obtained from the striation spectrum.

From figure 9(a) it is clearly seen that the three amplitudes decrease when the value of the cutting speed is increased. Also, the values of R_q and δ are from the same order whereas the values of R_z are 3 to 4 times larger. Here, it is also worthwhile to point out that the decrease of striation amplitudes with increasing focal position is linked to an increase of damping constants as seen in figure 8(b). This is consistent with the driven harmonic oscillator model and it is a strong hint that the striation dynamics is consistent with the model.

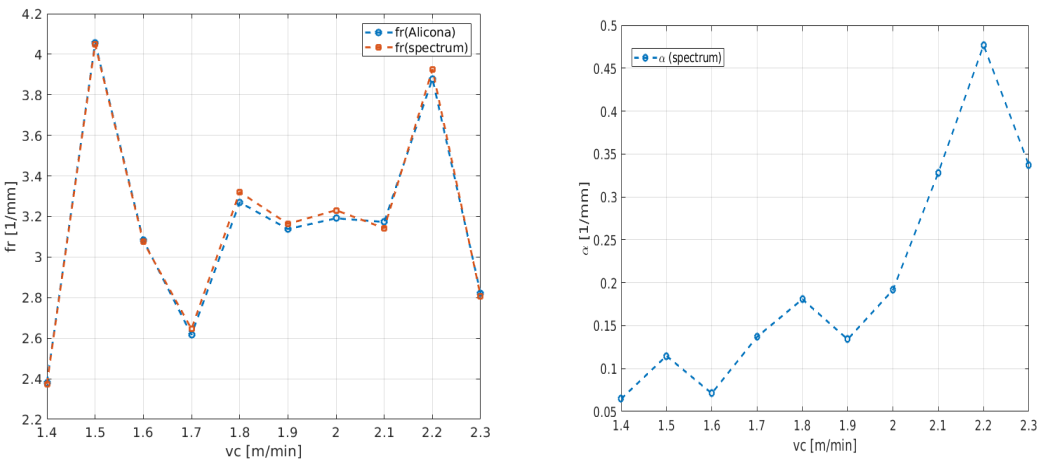

Fig. 8. (a) Striation spatial frequency; (b) Damping constant.

Figure 9(b) shows the striation amplitudes, i.e. the values of R_q, δ and δ (Model-formula) as function of the cutting speed. The value of δ was obtained from the striation spectrum by applying equation (3). The value of A_0 was obtained from the spectral analysis.

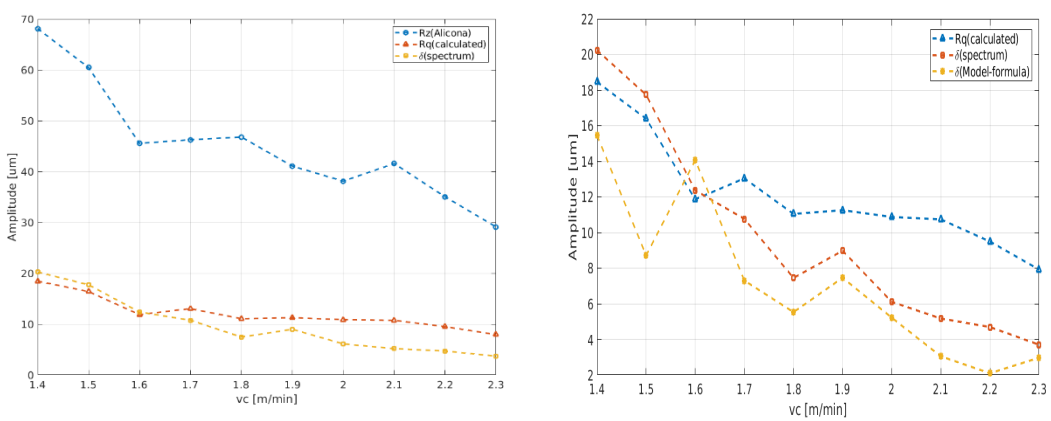

Fig. 9. (a) Striation spatial frequency; (b) Damping constant.

6. Conclusions

A rigorous spectral analysis of the measured roughness profiles produces results that are in a good agreement with our model of the reactive gas laser cutting process. As a result, this model can be used in the future to estimate quality factors such as spatial striation frequencies or striation amplitudes, i.e. roughness of the cut edge, in reactive gas assisted laser cutting.

Acknowledgement

This research was founded by Innosuisse (Project Number: 26112.1PFNM-NM).

References

[1] M. Vicanek, G. Simon, H. M. Urbassek, and I. Decker, "Hydrodynamical instability of melt flow in laser cutting," *J. Phys. D Appl. Phys.*, vol. 20, pp. 140–145, 1987.

[2] K. Chen and Y. L. Yao, "Striation formation and melt removal in the laser cutting process," *J. Manuf. Syst.*, vol. 18, no. 2, Supplement 1, pp. 43–53, 1999.

[3] G. V Ermolaev, O. B. Kovalev, A. M. Orishich, and V. M. Fomin, "Mathematical modelling of striation formation in oxygen laser cutting of mild steel," *J. Phys. D. Appl. Phys.*, vol. 39, no. 19, p. 4236, 2006.

[4] Y. Arata, H. Muruo, I. Milyamoto, and S. Takeuchi, "Dynamic behaviour in laser cutting of mild steel," *Jwri*, vol. 8, pp. 15–26, 1979.

[5] A. Ivarson, J. Powell, J. Kamalu, and C. Magnusson, "The oxidation dynamics of laser cutting of mild steel and the generation of striations on the cut edge," *J. Mater. Process. Tech.*, vol. 40, no. 3–4, pp. 359–374, 1994.

[6] D. Schuöcker, "Theoretical model of reactive gas assisted laser cutting including dynamic effects," in *Proc. SPIE 650, High Power Lasers and Their Industrial Applications (1986)*, 1986, vol. 650, pp. 210–219.

[7] D. Schuöcker, "Dynamic phenomena in laser cutting and cut quality," *Appl. Phys. B*, vol. 40, no. 1, pp. 9–14, 1986.

[8] K. Hirano and R. Fabbro, "Possible explanations for different surface quality in laser cutting with 1 and 10 µm beams," *J. Laser Appl.*, vol. 24, no. 1, pp. 12001–12006, 2012.

[9] W. M. Steen, *Laser Material Processing*, Second edition. Springer-Verlag London, 1991.

[10] R. Poprawe, "Modeling, Monitoring and Control in High Quality Laser Cutting," *CIRP Ann. - Manuf. Technol.*, vol. 50, no. 1, pp. 137–140, 2001.

[11] J. Dowden. (Ed.), *The Theory of Laser Materials Processing*. P.O. Box 17, 3300 A A Dordrecht, The Netherlands: Springer Science+Business Media B.V., 2009.